Herschel Science Centre

Pointing Updates in HCSS 13.0 – Description and performance

Compiled by Miguel Sánchez-Portal

Document No: HERSCHEL-HSC-DOC-2086

Version: 1.0 Draft

January 24, 2015

Document history

Date	Issue	Pages	Reason for Change
January 24 2015	1.0 Draft	All	First version

Contents

1 Introduction

This document summarises the pointing updates included in HCSS 13.0 and the main results of the tests performed so far.

1.1 Acronyms

The following acronyms are used throughout the document:

Acronym	Meaning
AOR	Astronomical Observation Request
APE	Absolute Pointing Error
HIPE	Herschel Interactive Processing Environment
HSC	Herschel Science Centre
ICC	Instrument Control Centre
MIPS	Multi-Band Imaging Photometer for *Spitzer*
PACS	Photodetector Array Camera and Spectrometer
PEP	PACS Evolutionary Probe; a Guaranteed Time Key Programme (P.I. D. Lutz)
PSF	Point-Spread Function
PT–AI	Pointing Tools – Attitude Improvement Software
RPE	Relative Pointing Error
SPG	Standard Pipeline Processing
SRPE	Spatial Relative Pointing Error
SVV	Spacecraft Velocity Vector

2 New functionality added

The main functions added to HCSS 13.0 in the pointing area are related to the ground-processed attitude using gyroscopes. The original software produced by the PACS ICC and included in the `toolbox.pointing` package since HCSS 12 has been further improved at the HCS, on the one hand, and on the other, ported from jython to java and included in the auxiliary processor that creates the pointing product in order to produce the improved attitude estimates as part of the standard product generation (SPG) process. The software is thoroughly described in [RD.1]. In addition, some changes have been incorporated to the pointing product (see sect. 3).

In addition, other minor changes have been incorporated. The most important one is the inclusion in the SPG of the special processing required to handle special operations events affecting pointing, namely STR switch-overs and SVV resets.

ToDo: add some more detailed description of the software items included in the new release.

Note: hereafter, simple-processed attitude refers to that ecomputed on-ground based on the naïve improvement algorithm, i.e. that correcting the filtered attitude information computed on-board for the systematic, though position-dependent, STR offets.

3 Updates to the pointing product

The updates to the pointing product are throughly described in [RD.2]. The changes include:

- A new column holding the simple-corrected attitude quaternion. The "filtered attitude" now contains the most accurate ground-processed estimate, namely the gyro-reconstructed attitude.
- 6 quality estimation columns for the gyro-reconstructed attitude.
- A new column, `filterQuatFlag` containing a flag related to the origin of the contents of the filtered quaternion field.
- A new meta-datum added to indicate the STR in use.

4 Results of the tests performed

The tests described below were designed to verify the function and performance of the gyro-based ground processing functionality incorporated to HCSS 13.0. This software was primarily aimed at improving the on-ground knowledge of the high-frequency changes of the spacecraft attitude (known as RPE, pointing stability or spacecraft jitter). However, it has been observed a general improvement of the spacecraft attitude, including the absolute pointing accuracy (measured by the APE) and the pointing stability (RPE).

The tests have been performed with HCSS 13.0 build id. 4309. The details of the methodology and set-up of the tests are given in [AD.1].

4.1 Absolute pointing error – Point source mode

We have processed all the pointing calibration observations carried out in the PACS photometer point-source mode and the "blue" camera with the 70 mum filter for the whole mission but for the OD range 866–1010. The results are summarised in the table 1. It can be seen that the absolute pointing accuracy as given by the APE[†] (as defined in [RD.3]) improves with the gyro-based processing for all periods but for the last one, where all the STR focal plane corrections were already available on-board. On the other hand, the distribution of Y/Z offsets is well behaved, as expected for random pointing errors, as seen in figures 1–4.

Table 1: Summary of absolute pointing accuracy results. Point-source mode.

OD range	Raw accuracy APE† (arcsec)	simple-processed APE† (arcsec)	gyro-based APE† (arcsec)	number of observations
32–320	1.9–2.2	1.4	1.4	356
321–761	2.4[a]	1.6	1.2	280
762–865	1.45	1.3	1.2	169
866–1010	1.1	–	N/A	–
1011–1452 (EoH)	0.9	–	1.2	182

[a]extreme outliers at ≥ 8 arcsec possible

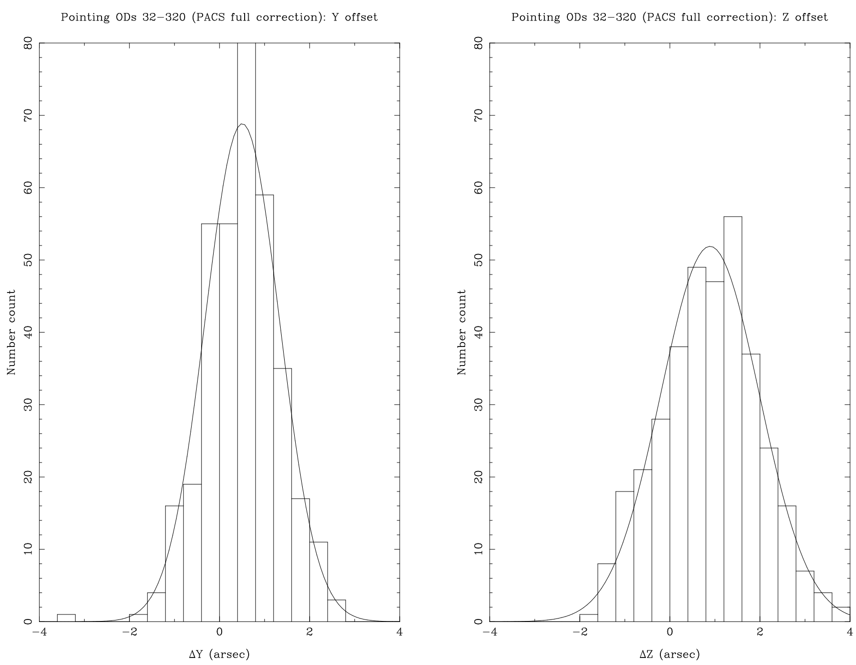

Figure 1: Y and Z distributions of offsets: OD 32–320

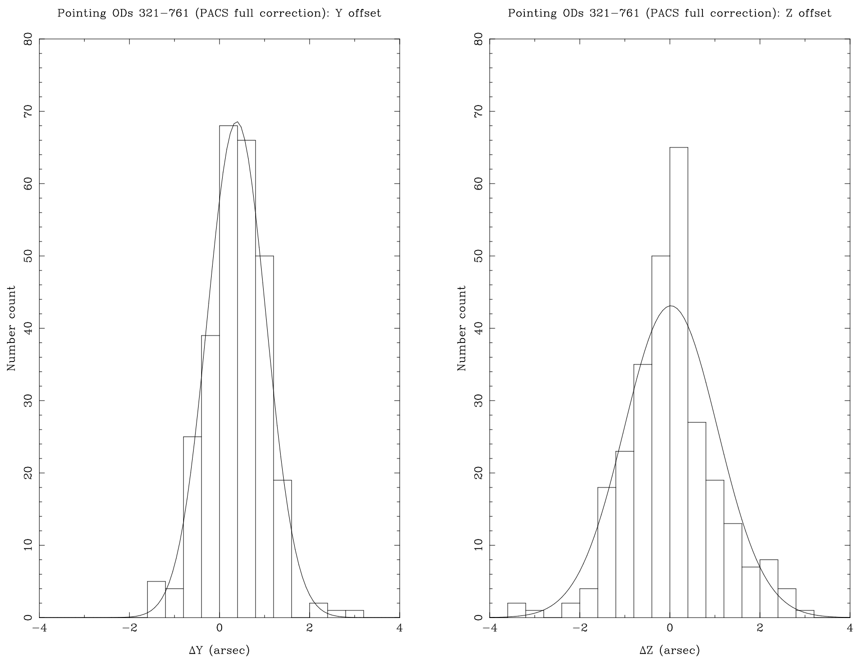

Figure 2: Y and Z distributions of offsets: OD 321–761

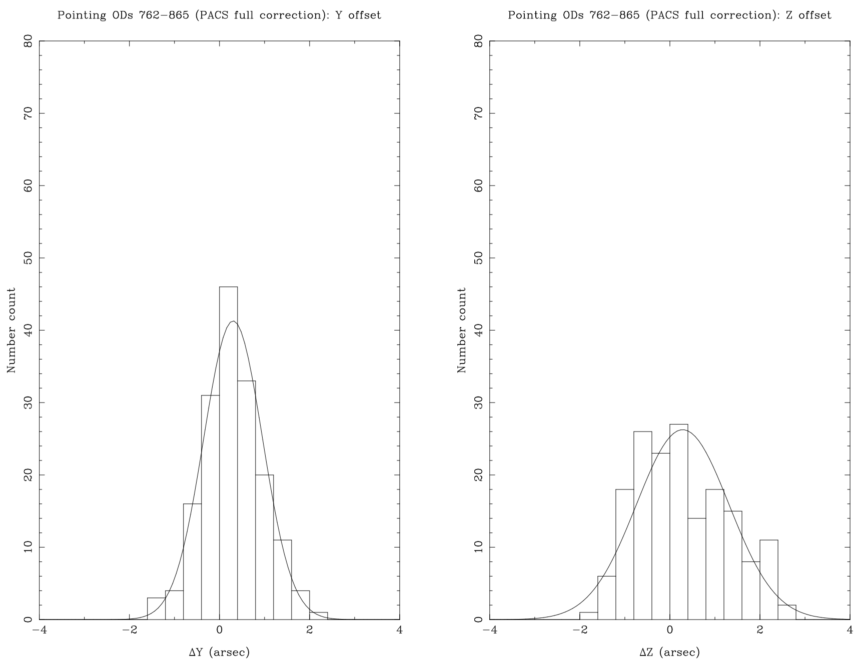

Figure 3: Y and Z distributions of offsets: OD 762–865

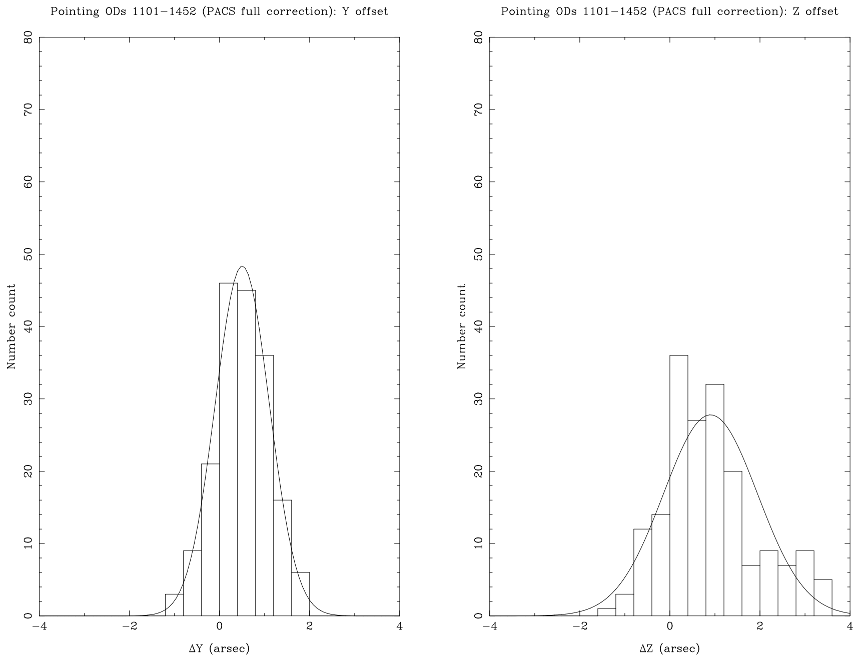

Figure 4: Y and Z distributions of offsets: OD 1011–1452

We have also measured the offset between the gyro-reconstructed and the simple-reconstructed attitude for these observations. The distribution of the offsets between the gyro and 'simple' attitudes is scattered as expected around (0,0) and has a dispersion that depends on the considered epoch, as shown in table 2.

Table 2: Offsets between simple- and gyro-processed attitude estimates. Point source mode.

OD range	$\langle \Delta RA \rangle$ (arcsec)	$\langle \Delta DEC \rangle$ (arcsec)	$\sigma_{gyro-simple}$ (arcsec)
32–320	0.00	0.00	1.30
321–761	-0.14	0.03	1.30
762–865	0.03	0.15	0.74
1011–1452	-0.14	-0.03	0.66

The results indicate that the scatter of offsets is reduced in the last period of the mission, where the simple-processed correction was small (in OD 762–865 it was just a an additional offset from the 1-D to the 2-D linear STR focal length correction) or none (OD 1101–1452) since the corrections were already included in the STR on-board.

The distribution of scatter of the offsets is depicted in figure 5. Random directions of the scatters ar observed, as expected.

However, the distribution of RA and DEC offsets shows some correlation in the the first two periods of the missions as depicted in figure 6, while it was not noticeable in the later ones, as shown in the two attached plots. This suggests that the offsets were induced by the some marginal systematic effect induced by the 'simple' correction (this was already expected, after all the correction was rather crude) and that the systematic effect dissapeared once the correction was already on-board.

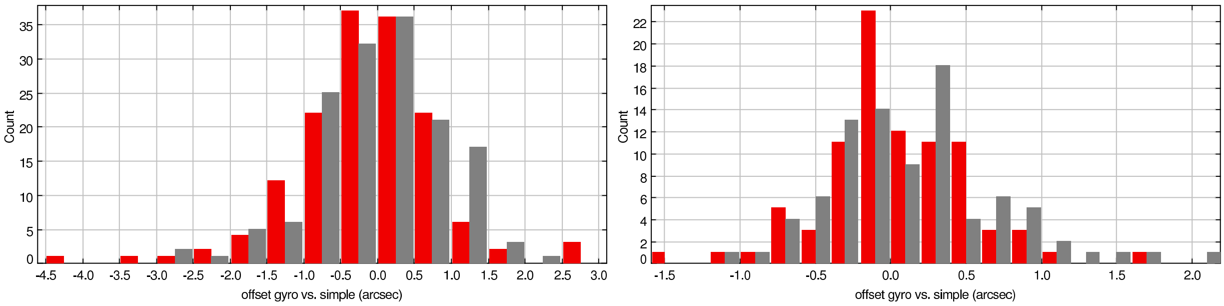

Figure 5: Histogram of the distribution of offsets of gyro- vs. simple-processed attitudes in RA (red) and DEC (green) for two periods within the mission: OD 321–761 (left) and 762–865 (right)

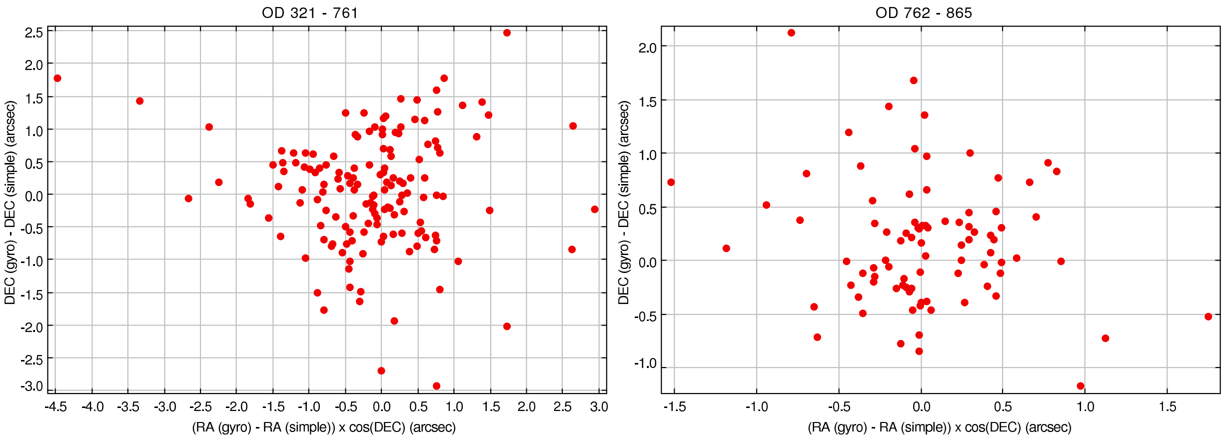

Figure 6: Distribution of offsets of gyro- vs. simple-processed attitudes in the RA/DEC space for two periods within the mission: OD 321–761 (left) and 762–865 (right). Some correlation between RA and DEC offsets is observed in the former period, that is absent or much weaker in the second one.

4.2 Absolute pointing error – Scan map mode

A number of pointing calibration observations have been performed in scan map mode (PACS-P "mini-map" mode). A total of 160 observations have been retrieved from the HSA. From these, 5 observations showed particularly large offsets when processed in both gyro-based and simple ground processing. One observation (1342213246) was correctly processed using the simple algorithm but presented a large offset when processed with the gyro-based one. For the rest of observations (154) the results are shown in table 3. The PSF fit was performed with a circular two-dimensional Gaussian function. The number of observations was 71 in the period OD 607–748 and 83 in the period 1076–1266. Type "G" corresponds to gyro-based ground processing and "S" to simple ground processing. It can be observed that a slight-to-moderate improvement is observed in both absolute pointing accuracy (as measured by the APE†) and pointing stability (as indicated by the PSF size σ_{PSF}). This improvement can be noticed y both periods, not only in the 607–748 one, where the effect of the STR-induced offsets was maximum, but also in the range 1076–1266, where all the STR corrections where already up-loaded to the prime STR and hence no simple ground correction was longer required. This (unlike the results from point-source observations) suggests that some improvement can be achieved with ground processing even in the last part of the mission, at least for scan map observations.

Table 3: Results from pointing scan map observations.

OD range	Type (G/S)	$\langle \Delta Y \rangle$ (arcsec)	$\langle \Delta Z \rangle$ (arcsec)	APE† (arcsec)	σ_{PSF} (arcsec)
607–748	G	0.42	0.18	1.31	2.33
607–748	S	0.57	0.35	1.58	2.40
1076–1266	G	0.46	1.06	1.12	2.35
1076–1266	S	0.54	1.22	1.28	2.37

These results agree with those performed by the PACS ICC (refs. from D. Lutz and M. Nielbock). Some additional tests are currently on-going at the HSC with large scan maps.

4.3 Pointing stability

The gyro-processing software was primarily designed to improve the on-ground knowledge of the pointing stability or spacecraft jitter. Therefore, it was assumed that an outstanding improvement of the telescope PSF at any wavelength should be achieved.

We have performed an etimation of the improvement in the PSF by fitting 2-dimensional Gaussian distributions to the pointing calibration stars observed in both point source modes (the results for scan-map mode are shown in sect. 4.2); these stars have strong, purely photospheric FIR flux densities, chosen in order to ensure that their FIR emission was as compact as possible (no dust shells), i.e. true "point sources". The distribution of PSFs derived from the observations processed with the improved pointing products and the standard ones have been compared (average PSF width and dispersion of data).

The results are shown in tables 4 and 3. It can be observed a exceptional stability of the measurements across all the studied periods. The PSF widths and dispersions are very similar from both gyro- and simple- processed attitude estimates, being marginally better those obtained from gyro-processed attitude.

Table 4: PSF estimates from simple- and gyro-processed attitude. Point source mode.

OD range	Type (G/S)	$\langle\sigma_{PSF,X}\rangle$ (arcsec)	$\sigma(\sigma_{PSF,X})$ (arcsec)	$\langle\sigma_{PSF,Y}\rangle$ (arcsec)	$\sigma(\sigma_{PSF,Y})$ (arcsec)
32–320	G	2.67	2.41	0.20	0.18
32–320	S	2.74	2.43	0.26	0.18
321–761	G	2.67	2.41	0.23	0.20
321–761	S	2.73	2.44	0.26	0.20
762–865	G	2.66	2.40	0.23	0.17
762–865	S	2.74	2.43	0.23	0.17
1011–1452	G	2.69	2.42	0.17	0.16
1011–1452	S	2.76	2.46	0.20	0.17

References

[RD.1] Stephenson, C.: "Guide to the Herschel Gyro-based Attitude Reconstruction Software", HERSCHEL-HSC-TN-2069, Draft, Rev. B, 11 June 2014

[RD.2] Sánchez-Portal, M.: "Herschel Pointing Product Specification", HERSCHEL-HSC-DOC-0662, v1.15, 16 December 2014.

[RD.3] Sánchez-Portal, M., Marston, A., Altieri, B., et al. 2014, Experimental Astronomy, 37, 453

[AD.1] Sánchez-Portal, M.: "Test Plan – Pointing Toolbox Attitude Improvement Software", HERSCHEL-HSC-DOC-2071, v1.0 Draft, 30 June 2014.